Nonrenewal resetting of scaled Brownian motion

Anna S. Bodrova,[1,2,3,*] Aleksei V. Chechkin,[4,5] and Igor M. Sokolov[1]

[1]*Department of Physics, Humboldt University, Newtonstrasse 15, 12489 Berlin, Germany*

[2]*Moscow Institute of Electronics and Mathematics, National Research University Higher School of Economics, Moscow 123458, Russia*

[3]*Faculty of Physics, M. V. Lomonosov Moscow State University, Moscow 119991, Russia*

[4]*Institute of Physics and Astronomy, University of Potsdam, 14476 Potsdam, Germany*

[5]*Akhiezer Institute for Theoretical Physics, Kharkov Institute of Physics and Technology, 61108 Kharkov, Ukraine*

(Received 13 December 2018; revised manuscript received 24 May 2019; published 15 July 2019)

We investigate an intermittent stochastic process in which diffusive motion with a time-dependent diffusion coefficient, $D(t) \sim t^{\alpha-1}$, $\alpha > 0$ (scaled Brownian motion), is stochastically reset to its initial position and starts anew. The resetting follows a renewal process with either an exponential or a power-law distribution of the waiting times between successive renewals. The resetting events, however, do not affect the time dependence of the diffusion coefficient, so that the whole process appears to be a nonrenewal one. We discuss the mean squared displacement of a particle and the probability density function of its positions in this process. We show that scaled Brownian motion with resetting demonstrates rich behavior whose properties essentially depend on the interplay of the parameters of the resetting process and the particle's displacement infree motion. The motion of particles can remain almost unaffected by resetting but can also get slowed down or even be completely suppressed. Especially interesting are the nonstationary situations in which the mean squared displacement stagnates but the distribution of positions does not tend to any steady state. This behavior is compared to the situation [discussed in the companion paper; A. S. Bodrova *et al.*, Phys. Rev. E **100**, 012120 (2019)] in which the memory of the value of the diffusion coefficient at a resetting time is erased, so that the whole process is a fully renewal one. We show that the properties of the probability densities in such processes (erasing or retaining the memory on the diffusion coefficient) are vastly different.

DOI: 10.1103/PhysRevE.100.012119

I. INTRODUCTION

Resetting represents a class of stochastic processes in which a random motion is from time to time terminated and restarted from given initial conditions. The instant of restarting can depend on the state of the process (e.g., it may be restarted under level crossing, as in many neuronal models [1]) or may be independent of this. The latter class of processes (motion under stochastic resetting) is what we consider here. One of the first studies of processes with resetting was devoted to a discrete-time stochastic multiplicative model [2].

The random motion under stochastic resetting arises as the interplay of two distinct random processes: the resetting process, a point process on the real line representing the time axis; and the particle's motion between resetting events, which we call the displacement process. The first work in the direction we follow in the present paper concentrated on the case where the displacement process is an ordinary Brownian motion [3], i.e., a Markovian process with stationary increments. The same is true for Lévy flights considered in [4] and [5], where, differently from Brownian motion, the trajectories of the free displacement process are discontinuous. Starting from the one-dimensional Brownian motion of single particles with resetting to the initial position [3,6], the process was further generalized to two and more dimensions [7] and to motion in a bounded domain with reflecting [8] and adsorbing [9] boundaries and in an external potential [10,11]. Also, cases with several choices of resetting position [12–14], with nonstatic restart points [15], and with several interacting Brownian particles with resetting [16] were discussed. Resetting has been investigated in the context of reaction diffusion with stochastic decay rates [17] and branching processes [18,19]. Large deviations and phase transitions for Markov processes under resetting were considered in Ref. [20].

Stochastic resetting of a diffusion process fundamentally changes its properties due to competition between the tendency toward diffusive spreading and repeated returns to the initial state. The ordinary normal diffusion process interrupted at a constant rate by resetting to the initial position [3] generates a nonequilibrium stationary state (NESS). However, the limitation to a constant resetting rate severely restricts the applicability to memoryless resetting processes. The more general case of gamma and Weibull distributions of waiting times between resetting events was discussed in [21]. Resetting with a position-dependent resetting rate [12] and with a time-dependent resetting rate [22] and resetting with a power-law distribution of waiting times between resetting events [23] have also been considered. Resetting-induced NESS has also been studied in many-body systems such as coagulation-diffusion processes [24].

Another important direction of work is connected with investigations on non-Markovian processes with resetting. Thus, Ref. [25] discusses resetting of a particle to a position

*bodrova@polly.phys.msu.ru

chosen from its trajectory in the past according to some memory kernel. Another displacement process with memory considered corresponds to a continuous-time random walk (CTRW) with or without drift [26–29].

In the present paper we consider scaled Brownian motion (SBM) with stochastic resetting. SBM is a paradigmatic Gaussian process governed by the overdamped Langevin equation with a diffusion coefficient which scales as a power law in time,

$$\frac{dx(t)}{dt} = \sqrt{2D(t)}\eta(t), \tag{1}$$

where $D(t) \simeq t^{\alpha-1}$ with $\alpha > 0$. Here $\eta(t)$ represents white Gaussian noise with zero mean $\langle \eta(t) \rangle = 0$ and covariance $\langle \eta(t_1)\eta(t_2) \rangle = \delta(t_1 - t_2)$. Setting

$$D(t) = \alpha K_\alpha t^{\alpha-1}, \tag{2}$$

one gets the mean squared displacement (MSD),

$$\langle x^2(t) \rangle = 2K_\alpha t^\alpha. \tag{3}$$

For $0 < \alpha < 1$ the motion is subdiffusive, and for $\alpha > 1$ one speaks about superdiffusion [30–37]. The case $\alpha = 2$ corresponds to ballistic spread, and cases with $\alpha > 2$ are termed superballistic or hyperdiffusive. In the limiting case $\alpha = 0$ the diffusion process is ultraslow with logarithmic time dependence of the MSD [38]. We note that the underdamped Langevin equation with a time-dependent diffusion coefficient has been studied in [39] and [40].

SBM as a model for anomalous diffusion was first introduced by Batchelor to model turbulent dispersion [41], where the particles' spread is described by Richardson's law [42] with the exponent $\alpha = 3$. Interestingly enough, the alternative models were Lévy flights (introduced long before the name was coined; see Sec. 24.4 of Ref. [43]) and Lévy walks [44].

SBM was used to describe fluorescence recovery after photobleaching in various settings [45], as well as anomalous diffusion in various biophysical contexts including brain matter [46,47]. A time-dependent diffusion coefficient may be observed in systems with a time-dependent temperature, such as melting snow [48,49] or free cooling granular gases [50–52]. A granular gas of viscoelastic particles represents an illuminating example of a many-particle system where the self-diffusion follows subdiffusive SBM with $\alpha = 1/6$; for a granular gas of particles colliding with a constant restitution coefficient SBM with $\alpha = 0$ has been observed [53].

The very term scaled Brownian motion was introduced in Ref. [54], where the authors compare the properties of SBM and fractional Brownian motion (FBM). Both processes are Gaussian random processes with the same single-time probability density functions (PDFs) but are intrinsically different in many other respects. Thus, SBM is a Markovian process with nonstationary increments, whereas FBM is non-Markovian but possesses stationary increments (which always show regimes; see [54]). In contrast to FBM, SBM exhibits discordance between its ensemble and its time-averaged MSDs, which is a sign of ergodicity breaking [30]. The nonergodicity of SBM does not, however, go hand in hand with the strong difference between its different realizations: its heterogeneity (ergodicity-breaking) parameter tends to 0 for long trajectories [55].

In the subdiffusive case SBM can be considered a mean-field approximation for the CTRW model [56] with a power-law waiting-time PDF, which also has nonstationary increments. However, in SBM this nonstationarity is modeled via the explicit time dependence of the diffusion coefficient, while the CTRW, being of the renewal class, lacks explicit time dependences of its parameters. On the other hand, SBM is a Markovian process, while CTRW is a non-Markovian (semi-Markovian) one. Nevertheless, the aging properties of both processes are very similar.

Therefore, just like in the CTRW, two situations can be discussed: the dynamics of the underlying process is rejuvenated after resetting or is not influenced by the resetting of the coordinate. In the CTRW the first assumption would mean that a new waiting period starts immediately after the resetting event; see [28] for a discussion of the corresponding physical assumptions. In the second situation the waiting period started before the resetting event is not interrupted by the resetting. Reference [28] concentrated on the first situation, corresponding to the renewal property of the whole process.

In SBM the first assumption corresponds to the situation where the diffusion coefficient also resets to its initial value, while another situation corresponds to the case where only the position of the particle is altered by the resetting events and the diffusion coefficient remains unaffected. The two situations are quite different in their behavior. In the present work we concentrate the nonrenewal situation while the fully renewal one, is considered in the companion paper [57]. We analytically derive the MSD and PDF for the cases of exponential and power-law resetting and compare our predictions with the results of numerical simulations.

We proceed as follows. In Sec. II we define the main quantities describing the behavior of the system with resetting and describe the details of numerical simulation. In Secs. III and IV we give the analytic results for SBM with exponential and power-law resetting, respectively, and compare them with the numerical simulations. Finally, we give our conclusions in Sec. V.

II. STOCHASTIC RESETTING

Let us consider a particle returning to the initial position $x = 0$ at random times. We denote by $\psi(t)$ the probability density function of waiting times between two consecutive resetting events. In the present work we concentrate on two cases: the first one is when this PDF is exponential (which corresponds to a Poissonian resetting process), $\psi(t) \sim e^{-rt}$; in the second one it follows a power law, $\psi(t) \sim t^{-1-\beta}$. The survival probability $\Psi(t)$ gives the probability that no resetting event occurs between 0 and t,

$$\Psi(t) = 1 - \int_0^t \psi(t')dt' = \int_t^\infty \psi(t')dt'. \tag{4}$$

Sometimes, especially for the case of a power-law PDF, it is convenient to switch between the time and the Laplace domains. The Laplace transform of the resetting PDF is

$$\tilde{\psi}(s) = \int_0^\infty \psi(t)\exp(-ts)dt. \tag{5}$$

The Laplace transform of the survival probability can be expressed via $\tilde{\psi}(s)$ as

$$\tilde{\Psi}(s) = \frac{1-\tilde{\psi}(s)}{s}. \tag{6}$$

The probability density $\psi_n(t)$ that the nth resetting event happens at time t satisfies the renewal equation [31]

$$\psi_n(t) = \int_0^t \psi_{n-1}(t')\psi(t-t')dt', \tag{7}$$

and the sum of all $\psi_n(t)$ gives the rate of resetting events at time t:

$$\kappa(t) = \sum_{n=1}^{\infty} \psi_n(t). \tag{8}$$

Its Laplace transform yields

$$\tilde{\kappa}(s) = \sum_{n=1}^{\infty} \tilde{\psi}^n(s) = \frac{\tilde{\psi}(s)}{1-\tilde{\psi}(s)}. \tag{9}$$

The probability of finding the particle at location x at time t (PDF) is

$$p(x,t) = \Psi(t)p_0(x,t,0) + \int_0^t dt'\kappa(t')\Psi(t-t')p_0(x,t,t'). \tag{10}$$

Here the first term accounts for the realizations where no resetting took place up to the observation time t. The weight of such realizations in the ensemble of all realizations is given by $\Psi(t)$. The second term accounts for the case where the last resetting event before the observation occurs at time t' [the probability of which is $\kappa(t')dt'$], no resetting occurs between t' and t, and the particle moves freely between these two instants in time. The first term may be safely neglected at long times $t \to \infty$, and the PDF of the particle's positions at such long times is

$$p(x,t) \simeq \int_0^t dt'\kappa(t')\Psi(t-t')p_0(x,t,t'). \tag{11}$$

Between t' and t the particle performs free SBM with the PDF given by

$$p_0(x,t,t') = \sqrt{\frac{1}{4\pi K_\alpha (t^\alpha - t'^\alpha)}} \exp\left(-\frac{x^2}{4K_\alpha(t^\alpha - t'^\alpha)}\right). \tag{12}$$

Multiplying Eq. (10) by x^2 and performing integration over x, we get the equation for the MSD of particles:

$$\langle x^2(t)\rangle = 2K_\alpha t^\alpha \Psi(t) + 2K_\alpha \int_0^t dt'\kappa(t')\Psi(t-t')(t^\alpha - t'^\alpha). \tag{13}$$

At long times $t \to \infty$ the first term may be neglected and we obtain for the MSD

$$\langle x^2(t)\rangle \simeq 2K_\alpha \int_0^t dt'\kappa(t')\Psi(t-t')(t^\alpha - t'^\alpha). \tag{14}$$

The MSD may or may not be determined by the form of the PDF in the bulk and has to be calculated separately: A very peculiar situation corresponding to such a case, where the MSD stagnates but the bulk of the distribution shrinks, appears for power-law waiting-time distributions with $1 < \beta < 2$.

In what follows we obtain the PDF, Eq. (10), and the MSD, Eq. (13), for exponential and power-law resetting waiting-time densities for long times analytically and compare them to the results of numerical simulations. The event-driven simulations are performed as follows. For a given sequence of output times t we simulate the sequence of resetting events, find the time of the last resetting event $t' < t$, and set $x(t) = 0$. Then the position of the particle at time t is distributed according to a Gaussian with zero mean and variance, $\langle x^2(t)\rangle = 2K_\alpha(t^\alpha - t'^\alpha)$. The corresponding Gaussian can be obtained from a standard normal distribution generated using the Box-Muller transform. The results are averaged over $N = 10^4$ to 10^6 independent runs. In all our simulations K_α is chosen in such a way that $\alpha K_\alpha = 1$.

III. SCALED BROWNIAN MOTION WITH EXPONENTIAL RESETTING

The simplest and most studied case corresponds to exponentially distributed waiting times between resets:

$$\psi(t) = re^{-rt}. \tag{15}$$

In this case the resets occur at a constant rate r. The survival probability, according to Eq. (4), follows

$$\Psi(t) = e^{-rt}. \tag{16}$$

The rate at which resetting events follow is constant:

$$\kappa(t) = r. \tag{17}$$

This means that the resetting events occur with the same probability at any given interval dt of time.

A. Mean-squared displacement

The MSD for SBM with exponential resetting can be obtained by inserting Eqs. (16) and (17) into Eq. (13),

$$\langle x^2(t)\rangle = 2K_\alpha t^\alpha - 2K_\alpha r t^{1+\alpha} e^{-rt} \frac{M(\alpha+1,\alpha+2,rt)}{\alpha+1}, \tag{18}$$

where $M(a,b,z)$ is the Kummer function defined as [58]

$$M(a,b,z) = \frac{\Gamma(b)}{\Gamma(a)\Gamma(b-a)} \int_0^1 dt e^{zt} t^{a-1}(1-t)^{b-a-1}, \tag{19}$$

with $\Gamma(z)$ being the gamma function. Expanding the Kummer function $M(\alpha+1,\alpha+2,rt)$ for $rt \gg 1$ [58],

$$M(\alpha+1,\alpha+2,rt) = (\alpha+1)\frac{e^{rt}}{rt}\left[1 + O\left(\frac{1}{rt}\right)\right], \tag{20}$$

we get the power-law dependence for the MSD at long times,

$$\langle x^2(t)\rangle \simeq \frac{2\alpha K_\alpha}{r} t^{\alpha-1}. \tag{21}$$

The exponent in the time dependence of MSD is always smaller by 1 than in the case of free diffusive motion without resetting. In this way, resetting affects SBM in a similar way as putting the particle performing SBM into a confining harmonic potential [59] or in fractional Brownian motion in the

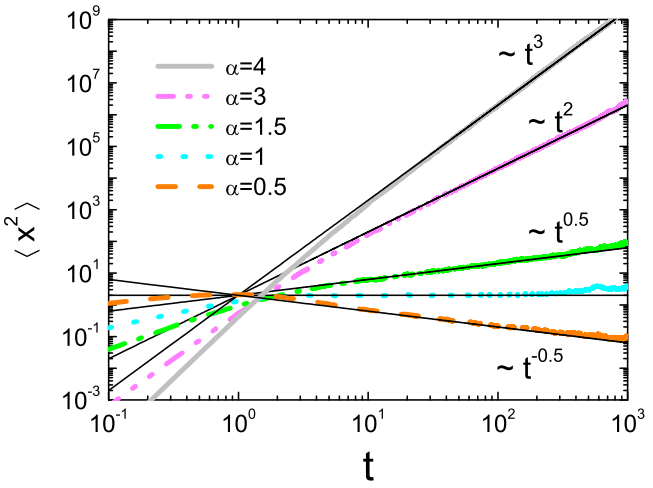

FIG. 1. The MSD for SBM with exponential resetting: theoretical results, Eq. (21) (thin solid black lines) and computer simulations (thick colored lines) obtained for $\alpha = 0.5$, 1, 1.5, 3, and 4.

fully renewal case [60]. For $\alpha = 1$, we reproduce the result for standard Brownian motion with exponential resetting, namely,

$$\langle x^2(t)\rangle = \frac{2K_1}{r}. \tag{22}$$

For ballistic motion between resetting events, $\alpha = 2$, the motion with resetting shows the MSD behavior akin to normal diffusion. Superdiffusive SBM with $1 < \alpha < 2$ becomes subdiffusive in the presence of resetting. The most interesting case corresponds to subdiffusive SBM, $0 < \alpha < 1$, where the MSD decays to 0 following a power law. This means that due to slowing-down of the motion over the course of time the particle is unable to get far away from the initial point between the resetting events and tends to remain in the vicinity of the origin.

The analytical result for the MSD in the case of exponential resetting, Eq. (21), has been compared with the numerical simulations, showing full agreement. In Fig. 1 we present the MSD for different values of α. The thick colored lines correspond to the numerical results; the thin solid lines correspond to asymptotics as given by Eq. (21). The light-gray line corresponds to initially superdiffusive motion with exponent $\alpha = 4$, which again turns to superdiffusion, but with the lower-power exponent $\alpha - 1 = 3$. For $\alpha = 3$ initially superdiffusive motion turns into ballistic motion with exponent $\alpha - 1 = 2$ (magenta line in Fig. 1). For $\alpha = 1.5$ initially superdiffusive motion turns into subdiffusion with $\alpha - 1 = 0.5$ in the presence of resetting (green line). In the case of ordinary diffusion with $\alpha = 1$ the MSD stagnates, as predicted in [3] (blue line). Initially subdiffusive motion with $\alpha = 0.5$ becomes trapped in the vicinity of the origin: the MSD tends to 0 as t^γ with $\gamma = \alpha - 1 = -0.5$ (orange line).

B. Probability density function

Let us now obtain the asymptotic form of the PDF for SBM with exponential resetting valid in the long-time limit for $t^{\alpha+1} \gg x^2/(K_\alpha r)$. Equation (11), together with Eqs. (12), (16), and (17), results in

$$p(x,t) \simeq r\int_0^t dt' \exp\left(-\frac{x^2}{4K_\alpha(t^\alpha - t'^\alpha)}\right)\frac{\exp(-r(t-t'))}{\sqrt{4\pi K_\alpha(t^\alpha - t'^\alpha)}}. \tag{23}$$

Using the new variable $\zeta = 1 - t'/t$ we rewrite Eq. (23) as

$$p(x,t) \simeq rt\int_0^1 d\zeta \frac{e^{\varphi(\zeta)}}{\sqrt{4\pi K_\alpha t^\alpha(1-(1-\zeta)^\alpha)}}, \tag{24}$$

where

$$\varphi(\zeta) = -rt\zeta - \frac{x^2}{4K_\alpha t^\alpha(1-(1-\zeta)^\alpha)}. \tag{25}$$

The major contribution to the integral, Eq. (24), comes from a small interval in the vicinity of $\zeta_{\max}$, where $\varphi(\zeta)$ attains its maximum, which is given by the solution of $\varphi'(\zeta_{\max}) = 0$. For x fixed and t large this maximum shifts closer and closer to 0, so that the approximation

$$1 - (1-\zeta_{\max})^\alpha \approx \alpha\zeta_{\max} \tag{26}$$

holds, and $\zeta_{\max}$ can be estimated as

$$\zeta_{\max} \simeq \sqrt{\frac{x^2}{4\alpha K_\alpha r t^{\alpha+1}}}. \tag{27}$$

The integral, Eq. (24), can then be evaluated using the standard Laplace method (i.e., expanding the argument of the exponential up to second order), thus giving

$$\begin{aligned} p(x,t) &\simeq \frac{rt}{\sqrt{4\pi K_\alpha t^\alpha \alpha\zeta_{\max}}} e^{\varphi(\zeta_{\max})}\int_{-\infty}^{\infty} d\zeta\, e^{-\frac{1}{2}(\zeta-\zeta_{\max})^2|\varphi''(\zeta_{\max})|} \\ &= \frac{rt e^{\varphi(\zeta_{\max})}}{\sqrt{2K_\alpha t^\alpha \alpha\zeta_{\max}|\varphi''(\zeta_{\max})|}}, \end{aligned} \tag{28}$$

with $\varphi''(\zeta_{\max})$ being the second derivative of φ at its maximum. Performing calculations we get

$$p(x,t) \simeq \frac{1}{2}\sqrt{\frac{r}{\alpha K_\alpha}}\, t^{\frac{1-\alpha}{2}} \exp\left(-\sqrt{\frac{r}{\alpha K_\alpha}}|x|t^{\frac{1-\alpha}{2}}\right). \tag{29}$$

This distribution is evidently non-Gaussian and time dependent and has a cusp at $x = 0$. For $\alpha = 1$, corresponding to ordinary Brownian motion, Eq. (29) tends to stationary steady state, obtained in [3]. In Fig. 2 we plot the PDF for initially subdiffusive SBM ($\alpha = 0.5$) under Poissonian resetting at different times. At short times $t < 1/r$ the width of the PDF is increasing, then it starts to decrease, collapsing, finally, to a vary narrow function. The initially subdiffusive motion leads over the course of time to trapping at the origin, as already seen from the behavior of its MSD, which at long times tends to 0 as t^γ with $\gamma = \alpha - 1 = -0.5$ (orange line in Fig. 1). In Fig. 3 the PDF for initially superdiffusive SBM ($\alpha = 3$) with Poissonian resetting is presented at different times, $t = 2$, 10, 100, and 1000. Here the distribution broadens rapidly and at longer times approaches the scaling form, as given by Eq. (29).

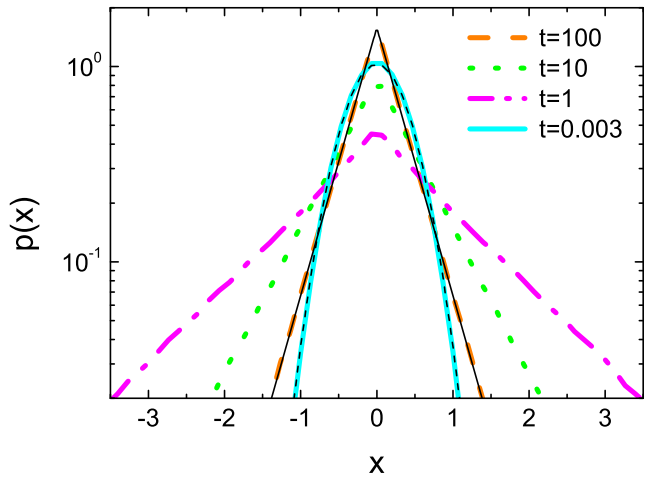

FIG. 2. The PDF for subdiffusive SBM ($\alpha = 0.5$) with Poissonian resetting for $t = 0.3$, 1, 10, and 100 (blue, magenta, green, and orange lines, respectively). The width of the PDF first is increasing and then starts to decrease. At the very short time $t = 0.003$ the PDF is Gaussian (light-blue line), reproducing the PDF of free SBM (thin dashed black line). At long times the PDF is described by Eq. (29) (thin solid black line).

IV. SCALED BROWNIAN MOTION WITH POWER-LAW RESETTING

Let us consider the case where the time between successive resets is distributed according to the power law

$$\psi(t) = \frac{\beta/\tau_0}{(1+t/\tau_0)^{1+\beta}}, \quad \beta > 0, \tag{30}$$

with τ_0 assumed to be constant, and is set to unity in simulations. The survival probability, according to Eq. (4), reads

$$\Psi(t) = (1+t/\tau_0)^{-\beta}. \tag{31}$$

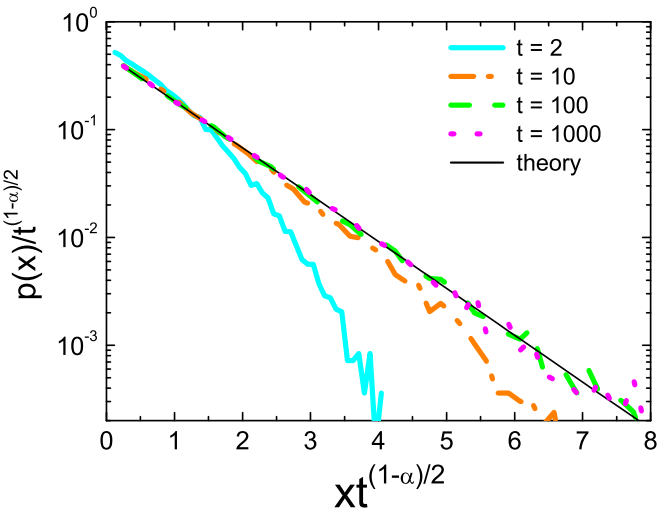

FIG. 3. The PDF for superdiffusive SBM ($\alpha = 3$) with Poissonian resetting as obtained in numerical simulations for $t = 2$, 10, 100, and 1000 (thick colored lines) and the prediction of the scaling form, Eq. (29).

For $\beta > 2$ both the first and the second moments of the distribution function of waiting times do exist:

$$\int_0^\infty t\psi(t)dt = \frac{\tau_0}{\beta-1}, \tag{32}$$

$$\int_0^\infty t^2\psi(t)dt = \frac{2\tau_0^2}{(\beta-1)(\beta-2)}. \tag{33}$$

For $1 < \beta < 2$ the second moment does not exist while the first moment does. For $\beta < 1$ both the first and the second moments diverge. As we see below the parameter β has a crucial impact on the behavior of the system.

In the Laplace domain

$$\tilde{\psi}(s) = \frac{\beta}{\tau_0}\int_0^\infty dt e^{-ts}\left(1+\frac{t}{\tau_0}\right)^{-1-\beta}. \tag{34}$$

Performing a change of the variables $y = s(t+\tau_0)$ and integrating by parts we get

$$\tilde{\psi}(s) = 1 - e^{s\tau_0}(s\tau_0)^\beta \int_{s\tau_0}^\infty dy e^{-y}y^{-\beta}. \tag{35}$$

For $s \to 0$ and $0 < \beta < 1$ the integration yields

$$\tilde{\psi}(s) = 1 - \Gamma(1-\beta)(s\tau_0)^\beta + \ldots. \tag{36}$$

For $1 < \beta < 2$ the asymptotic result for $s \to 0$ reads

$$e^{s\tau_0}\int_{s\tau_0}^\infty dy e^{-y}y^{1-\beta} \to \Gamma(2-\beta), \tag{37}$$

and we get

$$\tilde{\psi}(s) = 1 - \frac{s\tau_0}{\beta-1} + \frac{(s\tau_0)^\beta\Gamma(2-\beta)}{\beta-1} + \ldots, \tag{38}$$

while for $\beta > 2$ we get

$$\tilde{\psi}(s) = 1 - \frac{s\tau_0}{\beta-1} + \frac{(s\tau_0)^2}{(\beta-1)(\beta-2)} + \ldots, \tag{39}$$

with $0 < \beta < 1$, $1 < \beta < 2$, and $\beta > 2$.

A. $0 < \beta < 1$

1. *Mean squared displacement*

In order to calculate the MSD we use Eq. (14). The rate of the resetting events $\kappa(t)$ is given by Eq. (36) and Eq. (9),

$$\tilde{\kappa}(s) \simeq \frac{1}{\Gamma(1-\beta)\tau_0^\beta s^\beta}, \tag{40}$$

so that

$$\kappa(t) \simeq \frac{\tau_0^{-\beta}}{\Gamma(\beta)\Gamma(1-\beta)}t^{\beta-1}. \tag{41}$$

Unlike the case of exponential resetting, the rate of resetting events decays with time. The MSD for power-law resetting with $0 < \beta < 1$ can be obtained by inserting Eq. (41) into Eq. (14),

$$\langle x^2(t)\rangle \simeq 2K_\alpha t^\alpha\left(1 - \frac{1}{\alpha B(\alpha,\beta)}\right), \tag{42}$$

with $B(\alpha,\beta) = \int_0^1 dt t^{\alpha-1}(1-t)^{\beta-1} = \frac{\Gamma(\alpha)\Gamma(\beta)}{\Gamma(\alpha+\beta)}$ being the beta function. We note that $(1 - \frac{1}{\alpha B(\alpha,\beta)}) < 1$ so that the MSD

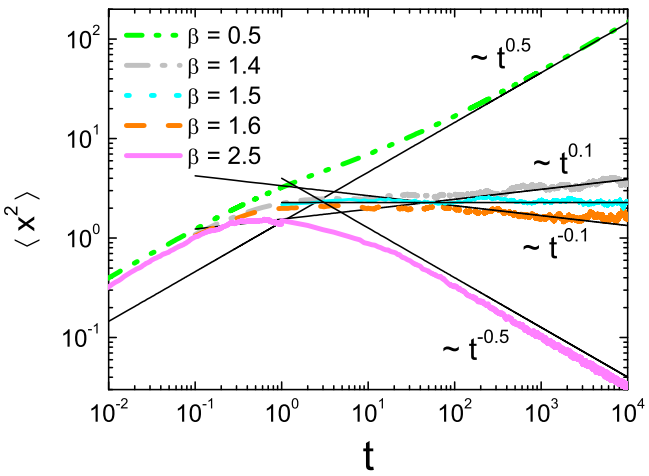

FIG. 4. The MSD for SBM with power-law resetting, $\alpha = 0.5$. This figure is referred to several times in the text. Thick colored lines correspond to numerical simulations. Thin solid black lines represent analytical results. For $\beta = 0.5$ Eq. (42) is used, for $\beta = 1.4$, 1.5, and 1.6 Eq. (58) is used, and for $\beta = 2.5$ Eq. (66) is used.

described by Eq. (42) differs from the MSD for a particle performing free diffusive SBM, Eq. (3), only by the prefactor: $\langle x^2(t)\rangle \simeq 2K_\alpha^* t^\alpha$ with $K_\alpha^* < K_\alpha$. The comparison between analytical and numerical results for power-law resetting is given in Fig. 4. Thick colored lines correspond to the numerical results, and dashed lines to the theory, showing the nice agreement in the asymptotic domain. Initially subdiffusive motion with $\alpha = 0.5$ remains subdiffusive: $\langle x^2\rangle \sim t^\alpha$ (green line corresponding to $\beta = 0.5$ in Fig. 4). Figure 4 gives an overview of all MSD behaviors under power-law resetting discussed in the present paper: Other lines in Fig. 4 show the results for the MSD for larger values of β as discussed below.

For $\alpha = 1$ expression (42) yields the normal diffusion regime with a different prefactor,

$$\langle x^2(t)\rangle \simeq 2K_1(1-\beta)t\,. \tag{43}$$

2. *Probability density function*

In order to calculate the PDF we consider the Fourier transform of Eq. (11):

$$\hat{p}(k,t) \simeq \int_0^t dt'\kappa(t')\Psi(t-t')\exp(-k^2K_\alpha(t^\alpha - t'^\alpha)). \tag{44}$$

For small k^2 (which correspond to large $|x|$ in the far tail of the distribution), $K_\alpha k^2 t^\alpha \ll 1$, one separates the exponentials containing t and t' and changes the variable of integration to $\tau = t'/t$:

$$\hat{p}(k,t) \simeq \frac{\exp(-K_\alpha k^2 t^\alpha)}{\Gamma(\beta)\Gamma(1-\beta)}\int_0^1 d\tau\,\tau^{\beta-1}(1-\tau)^{-\beta} \times \exp(K_\alpha k^2 t^\alpha \tau^\alpha). \tag{45}$$

The exponential in the integrand can then be approximated by unity, and the integration yields a constant value $B(\beta, 1-\beta)$, so that

$$\hat{p}(k,t) \simeq \exp(-K_\alpha k^2 t^\alpha). \tag{46}$$

The inverse Fourier transform gives the Gaussian behavior of the PDF in its far tail,

$$p(x,t) \simeq \frac{1}{\sqrt{4\pi K_\alpha t^\alpha}}\exp\left(-\frac{x^2}{4K_\alpha t^\alpha}\right). \tag{47}$$

This far-tail behavior is universal for power-law resetting.

For $K_\alpha k^2 t^\alpha \gg 1$ (which corresponds to x in the bulk of the distribution) one does not separate the exponentials and uses the approximation $\tau^\alpha \simeq 1 - \alpha(1-\tau)$. Introducing a new variable $\xi = 1 - \tau$ we find

$$\hat{p}(k,t) \simeq \frac{1}{\Gamma(\beta)\Gamma(1-\beta)}\int_0^1 d\xi\,\xi^{-\beta}(1-\xi)^{\beta-1}e^{-\alpha K_\alpha k^2 t^\alpha \xi}. \tag{48}$$

The upper limit of integration can then be shifted to infinity (since the argument of the exponential is very large and negative), and the inverse Fourier transform of this expression can be performed. The result for $x^2 \ll K_\alpha t^\alpha$ thus reads

$$p(x,t) \simeq \frac{1}{\Gamma(1-\beta)}\frac{1}{\sqrt{4\pi\alpha K_\alpha t^\alpha}} \times \exp\left(-\frac{x^2}{4\alpha K_\alpha t^\alpha}\right)U\left(\beta, \beta+\frac{1}{2}, \frac{x^2}{4\alpha K_\alpha t^\alpha}\right). \tag{49}$$

Here $U(a,b,z)$ is the Tricomi confluent hypergeometric function [58]

$$U(a,b,z) = \frac{1}{\Gamma(a)}\int_0^\infty dt e^{-zt}t^{a-1}(1+t)^{b-a-1}. \tag{50}$$

Using the expansion of $U(a,b,z)$ for $z \ll 1$ [58], we get the following asymptotics for Eq. (49):

$$p(x,t) \simeq \frac{1}{\sqrt{4\alpha K_\alpha t^\alpha \pi^2}}\sin(\pi\beta)\Gamma(1/2-\beta)\Gamma(\beta), \quad 0 \leqslant \beta < 1/2, \tag{51}$$

$$p(x,t) \simeq \frac{\Gamma(\beta-1/2)}{(4\alpha K_\alpha t^\alpha)^{1-\beta}}\frac{\sin(\pi\beta)}{\pi^{3/2}|x|^{2\beta-1}}, \quad 1/2 < \beta \leqslant 1. \tag{52}$$

This change in the behavior can be anticipated from the form of the integral defining the Tricomi function, Eq. (50), since for $\beta > 1/2$ the integral diverges at the upper limit for $z = 0$, while for $\beta < 1/2$ it converges at the upper limit also without the regularizing exponential depending on x, so that the distribution at small x develops a flat top. The transition involving logarithmic corrections is not captured by the asymptotic expansions.

For $\alpha = 1$ the PDF behaves as that for ordinary Brownian motion with power-law resetting with $0 < \beta < 1$ [23].

In Fig. 5 we show the results of numerical simulations for $\beta = 0.25$ at shorter times, which is indeed well fitted with the Gaussian function, Eq. (47). At variance with the case of subdiffusive SBM with exponential resetting, the width of the probability distribution increases.

In Fig. 6 the numerical results for the PDF for SBM with power-law resetting, $\beta = 0.75 > 1/2$, is shown. With rescaled variables $p(x,t)\sqrt{4\alpha K_\alpha t^\alpha}$ versus $x/\sqrt{4\alpha K_\alpha t^\alpha}$ the distribution functions at different times collapse and show nice agreement with the analytical solution, Eq. (52).

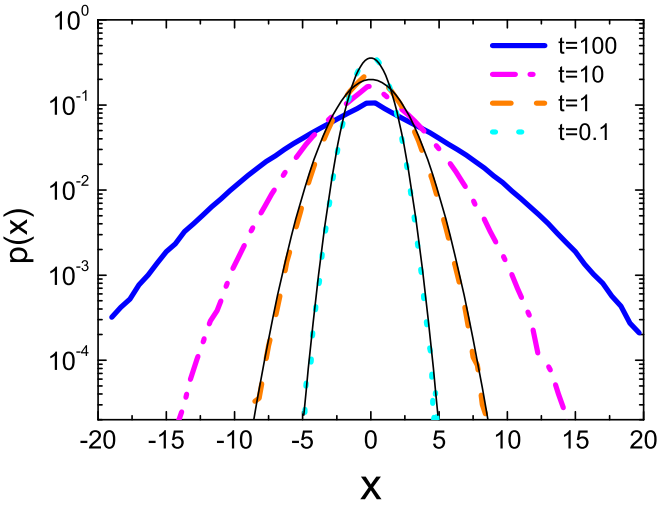

FIG. 5. The PDF for SBM with power-law resetting, $\beta = 0.25$, $\alpha = 0.5$, at times $t = 0.1$, 1, 10, and 100. Thin solid black lines show the Gaussians $\exp(-x^2/4K_\alpha t^\alpha)/\sqrt{4\pi K_\alpha t^\alpha}$, Eq. (47).

B. $1 < \beta < 2$

1. Mean squared displacement

The calculation leading to the MSD is similar to the case for $0 < \beta < 1$. We again use Eq. (14), but with a constant rate of resetting:

$$\kappa(t) \simeq \kappa = \frac{\beta - 1}{\tau_0}. \tag{53}$$

Plugging Eq. (53) into Eq. (14) results in

$$\langle x^2(t)\rangle \simeq \frac{2K_\alpha(\beta-1)}{\tau_0}\left[\int_0^t dt'\Psi(t-t')t'^\alpha - \int_0^t dt'\Psi(t-t')t'^{\alpha}\right], \tag{54}$$

with $\Psi(t)$ given by Eq. (31). The integration in the first term is straightforward. The second term has the form of a convolution, and the integral can be evaluated in the Laplace domain using

$$\tilde{\Psi}(s) \simeq \frac{\tau_0}{\beta-1} - \frac{\Gamma(2-\beta)s^{\beta-1}\tau_0^\beta}{\beta-1}, \tag{55}$$

as follows from Eq. (38) and Eq. (6), so that

$$\mathcal{L}\left\{\int_0^t dt'\Psi(t-t')t'^\alpha\right\} \simeq \frac{\Gamma(\alpha+1)}{s^{\alpha+1}}\left(\frac{\tau_0}{\beta-1} - \frac{\Gamma(2-\beta)s^{\beta-1}\tau_0^\beta}{\beta-1}\right). \tag{56}$$

By taking the inverse Laplace transform of Eq. (56), we obtain

$$\int_0^t dt'\Psi(t-t')t'^\alpha \simeq \frac{\tau_0}{\beta-1}\left(t^\alpha - \frac{\Gamma(2-\beta)\Gamma(1+\alpha)t^{1-\beta+\alpha}\tau_0^{\beta-1}}{\Gamma(\alpha-\beta+2)}\right). \tag{57}$$

The final result reads

$$\langle x^2(t)\rangle \simeq 2K_\alpha t^{1+\alpha-\beta}\tau_0^{\beta-1}(\alpha B(\alpha, 2-\beta) - 1). \tag{58}$$

The system with $1 < \beta < 2$ demonstrates very rich behavior. The exponent of the time dependence of the MSD decreases by the amount $\beta - 1$ compared to the free motion. This amount changes from 0 for $\beta = 1$ to 1 for $\beta = 2$. For $\beta < 1 + \alpha$ the MSD increases with time, and in the opposite case, $\beta > 1 + \alpha$, it decays at long times, in which case the particles are unable to move far away from the origin. In the case of superdiffusion the motion of particles either remains superdiffusive, tends to ordinary diffusion, or becomes subdiffusive. In the case of subdiffusion the motion can either slow down or become suppressed. For $\beta = 1 + \alpha$ the MSD stagnates. This is, however, a very intriguing situation since, as we proceed to show, the stagnation of the MSD does not imply the existence of a NESS.

A comparison between numerical and analytical results for this case is also presented in Fig. 4. For $1 + \alpha > \beta$ the system remains subdiffusive but with a lower exponent (gray line corresponding to $\beta = 1.4$ in Fig. 4); for $\beta = 1 + \alpha$ the MSD stagnates as depicted in Fig. 4 (blue line corresponding to $\beta = 1.5$ in Fig. 4). For $1 + \alpha < \beta$ the MSD tends to 0 (orange line corresponding to $\beta = 1.6$ in Fig. 4). As the particle cannot move away from the origin, resetting events can drastically affect $\beta = 1 + \alpha$, leading to trapping.

In the case of ordinary Brownian motion with resetting the particle performs subdiffusive motion

$$\langle x^2(t)\rangle \simeq 2K_1\tau_0^{\beta-1}t^{2-\beta}\frac{\beta-1}{2-\beta}. \tag{59}$$

This expression can be directly obtained from Eq. (58) by taking $\alpha = 1$.

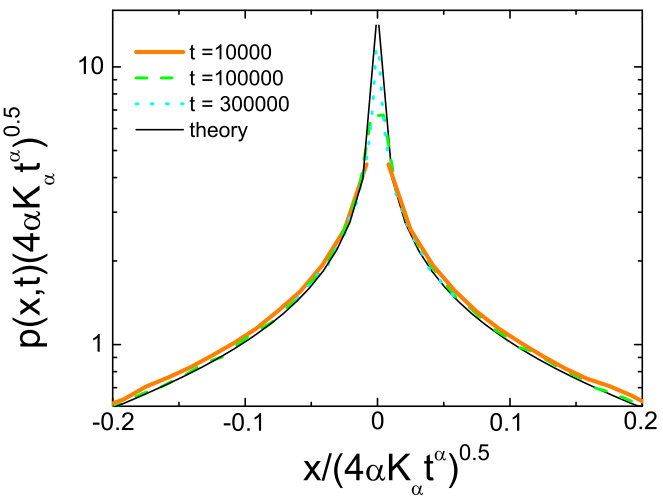

FIG. 6. The PDF for SBM with power-law resetting, $\beta = 0.75$, $\alpha = 0.5$, at long times. The thin solid black line represents Eq. (52).

2. Probability density function

Inserting the expressions for κ, Eq. (53), and $\Psi(t)$, Eq. (31), into Eq. (11) we get, in the time domain,

$$p(x,t) \simeq \frac{\beta-1}{\tau_0}\frac{1}{\sqrt{4\pi K_\alpha}}\int_0^t dt'\left(1+\frac{t-t'}{\tau_0}\right)^{-\beta}\frac{1}{\sqrt{t^\alpha - t'^\alpha}} \times \exp\left(-\frac{x^2}{4K_\alpha(t^\alpha - t'^\alpha)}\right). \quad (60)$$

Now we assume that $t \gg \tau_0$ and change the variable of integration to $y \simeq (1-(t'/t)^\alpha)^{-1}$:

$$p(x,t) \simeq \frac{t^{1-\beta-\frac{\alpha}{2}}\tau_0^\beta}{\alpha}\int_1^\infty dy y^{-\frac{1}{2}-\frac{1}{\alpha}}(y-1)^{\frac{1}{\alpha}-1}\left(1-\left(1-\frac{1}{y}\right)^{\frac{1}{\alpha}}\right)^{-\beta} \times \exp\left(-\frac{x^2 y}{4K_\alpha t^\alpha}\right). \quad (61)$$

For intermediate values of x (i.e., in the core of the PDF but not very close to its mode) the integral is dominated by large values of y, where we can make the approximations $(y-1)^{\frac{1}{\alpha}-1} \approx y^{\frac{1}{\alpha}-1}$ and $(1-(1-\frac{1}{y})^{\frac{1}{\alpha}})^{-\beta} \approx \alpha^\beta y^\beta$. The expression is now simplified to

$$p(x,t) \simeq t^{1-\beta-\frac{\alpha}{2}}\alpha^{\beta-1}\tau_0^\beta\int_1^\infty dy y^{\beta-\frac{3}{2}}\exp\left(-\frac{x^2 y}{4K_\alpha t^\alpha}\right). \quad (62)$$

The lower bound of integration may be safely shifted to 0, so that

$$p(x,t) \simeq \alpha^{\beta-1}\tau_0^\beta(4K_\alpha)^{\beta-\frac{1}{2}}\Gamma\left(\beta-\frac{1}{2}\right)t^{(\beta-1)(\alpha-1)}x^{1-2\beta}. \quad (63)$$

Omitting the prefactors we get

$$p(x,t) \sim x^{1-2\beta}t^{(1-\beta)(1-\alpha)}. \quad (64)$$

The distribution can be put into a scaling form, $p(x,t) = t^{-\gamma}f(x/t^\gamma)$ with $f(z) = z^{1-2\beta}$, so that $\gamma = (\alpha-1)/2$. This scaling form is shown in Fig. 7. For ordinary Brownian motion with power-law resetting and $\beta > 1$ the steady state $p(x,t) \sim x^{1-2\beta}$ is recovered [23].

Now we return to a balanced situation, $\beta = 1+\alpha$, when the MSD stagnates and see that the bulk of the distribution remains time dependent: the stagnation of the MSD is due to the compensation effect between the narrowing central peak and the growing tail, which is a quite peculiar situation, in no way representing a NESS.

At long times for parameter values $\beta = 1.25$, $\alpha = 0.5$ the PDF indeed follows the scaling predicted by Eq. (64) and has the asymptotic $p(x) \simeq x^{-3/2}$ as shown in Fig. 7.

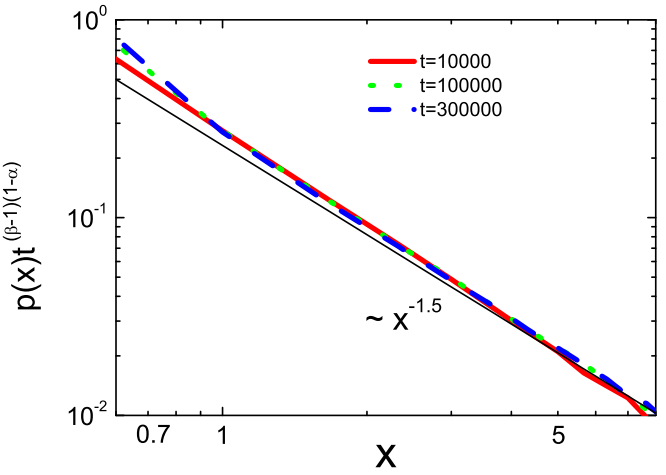

FIG. 7. The PDF for SBM with power-law resetting, $\beta = 1.25$, $\alpha = 0.5$, rescaled according to Eq. (64). Shown is $p(x)t^{(\beta-1)(1-\alpha)}$ as a function of x for $x > 0$. The thin black line has the slope $-3/2$ as follows from Eq. (64).

C. $\beta > 2$

1. Mean squared displacement

The MSD can be obtained similarly to that in the previous case, $1 < \beta < 2$. Inserting Eq. (39) into Eq. (6), we get for the Laplace transform of the survival probability

$$\tilde{\Psi}(s) \simeq \frac{\tau_0}{\beta-1} - \frac{s\tau_0^2}{(\beta-1)(\beta-2)}. \quad (65)$$

Now we can calculate the MSD using Eq. (54). The final form of the MSD reads

$$\langle x^2(t)\rangle \simeq \frac{2\alpha K_\alpha \tau_0}{\beta-2}t^{\alpha-1}. \quad (66)$$

This behavior resembles the MSD for Poissonian resetting [Eq. (21)]. Note that the exponent of the time dependence of the MSD, Eq. (66), ceases to depend on the exponent β of the waiting-time distribution; the dependence on β remains only in the prefactor. Nice agreement with the numerical simulation, shown as the magenta line corresponding to $\beta = 2.5$ in Fig. 4, is observed.

In the case of ordinary Brownian motion ($\alpha = 1$) the MSD stagnates:

$$\langle x^2(t)\rangle \simeq \frac{2K_1\tau_0}{\beta-2}. \quad (67)$$

2. Probability density function

The asymptotics for the PDF has the same form, Eq. (64), as for $1 < \beta < 2$.

TABLE I. Asymptotic behavior of the MSD and of the PDF in the intermediate domain of x for power-law resetting.

	$0 < \beta < 1/2$	$1/2 < \beta < 1$	$1 < \beta < 2$	$\beta > 2$
MSD	$\sim t^\alpha$	$\sim t^\alpha$	$\sim t^{\alpha+1-\beta}$	$\sim t^{\alpha-1}$
PDF	Flat top, Gaussian tail	$\sim t^{\alpha(\beta-1)}\lvert x\rvert^{1-2\beta}$	$\sim t^{(1-\beta)(1-\alpha)}\lvert x\rvert^{1-2\beta}$	$\sim t^{(1-\beta)(1-\alpha)}\lvert x\rvert^{1-2\beta}$

TABLE II. The MSD and PDF for renewal power-law resetting.

	$0 < \beta < 1 - \alpha/2$	$1 - \alpha/2 < \beta < 1$	$1 < \beta < 1 + \alpha$	$\beta > 1 + \alpha$
MSD	$\sim t^{\alpha}$	$\sim t^{\alpha}$	$\sim t^{\alpha+1-\beta}$	Stagnates
PDF	Flat top, Gaussian tail	$\sim t^{\beta-1}\lvert x\rvert^{-1-2\beta/\alpha+2/\alpha}$	$\sim \lvert x\rvert^{-1-2\beta/\alpha+2/\alpha}$	$\sim \lvert x\rvert^{-1-2\beta/\alpha+2/\alpha}$

V. CONCLUSIONS

In the present work we have discussed the MSD and the PDF for particles performing scaled Brownian motion with a time-dependent diffusion coefficient $D(t) \sim t^{\alpha-1}$ under resetting in a nonrenewal case, where the position of a particle is returned to the origin upon resetting, while the diffusion coefficient (changing with time) remains unaffected by the resetting events. The distribution of waiting times between two successive resetting events either is exponential, $\psi(t) \sim e^{-rt}$, or follows a power law, $\psi(t) \sim t^{-1-\beta}$. To the best of our knowledge, this is the first exhaustive study of a stochastic process which is not rejuvenated at a resetting event.

For $\beta < 1$ the power-law exponent of the MSD is not affected by resetting, $\langle x^2 \rangle \simeq t^{\alpha}$, but only changes the prefactor. For $1 < \beta < 2$ the MSD scales as $\langle x^2 \rangle \simeq t^{1+\alpha-\beta}$, and the behavior of the system is determined by the interplay of the exponents α and β, so that the particle's motion is either slowed down compared to free SBM or completely suppressed. Interestingly enough, the compensated case where the MSD stagnates does not correspond to a stationary state, since the PDF still changes with time.

The cases of Poissonian resetting and of power-law resetting with $\beta > 2$ show strong similarities in the behavior of the MSD: in both cases it scales as $\langle x^2 \rangle \simeq t^{\alpha-1}$. This means that such resetting always decreases the exponent of the MSD by unity, so that for $\alpha > 2$ the initially superdiffusive motion remains superdiffusive, for $1 < \alpha < 2$ superdiffusion tends to subdiffusion, and subdiffusive motion with $\alpha < 1$ becomes completely suppressed: the particles get trapped in the vicinity of the starting point.

Since SBM for $0 < \alpha < 1$ shows the same aging properties of the MSD as the CTRW, the very same behavior can be anticipated for resetting of the CTRW provided the resetting events do not rejuvenate the waiting times.

The PDF of the particle's position for nonrenewal resetting with an exponential waiting-time PDF is nonstationary but always shows a simple two-sided exponential (Laplace) shape. In the case of power-law resetting of a waiting-time PDF with very slow decay ($\beta < 1/2$) the PDF of positions does not show any universal scaling in the body and possesses Gaussian tails. In all other cases it tends to universal forms which differ in their time-dependent prefactor for $1/2 < \beta < 1$ and for $\beta > 1$. The behavior of the MSD and of the PDF in the bulk is reported in Table I.

These results should be compared with those for the situation where the transport process is rejuvenated under resetting, and the whole process is a renewal one, as discussed in detail in the companion paper [57]. The behavior observed in this renewal process significantly differs from the results discussed above. Here the behavior of the MSD is as follows: For exponential resetting and power-law resetting with $\beta > 1 + \alpha$ the MSD at long times stagnates. For $\beta < 1$ the time dependence of the MSD remains the same as in the case of free scaled Brownian motion, albeit with different prefactors. In the intermediate domain $1 < \beta < 1 + \alpha$ we obtain $\langle x^2 \rangle \sim t^{1+\alpha-\beta}$, so that the behavior of the MSD is defined by the interplay of the parameters α and β.

Turning to the behavior of the PDF we state that in the case of exponential resetting the PDF tends to a steady state with a stretched or squeezed exponential tail $p(x,t) \simeq \exp\left(-\gamma |x|^{\frac{2}{\alpha+1}}\right)$. For power-law resetting with $\beta > 1$ the PDF also attains a time-independent form, now $p(x,t) \sim x^{-1-\frac{2\beta}{\alpha}+\frac{2}{\alpha}}$. We note that for $\beta > 1 + \alpha$ both the MSD and the PDF tend to a stationary state, while for $1 < \beta < 1 + \alpha$ only the PDF in the bulk is stationary and the MSD increases continuously with time. For $\beta < 1$ the behavior of the PDF depends on the relation between the exponents β and α. For $\beta > 1 - \alpha/2$ the x dependence of the PDF for $\sqrt{4K_\alpha \tau_0^\alpha} \ll |x| \ll \sqrt{4K_\alpha t^\alpha}$ is the same as in the previous case, but now time dependence also appears: $p(x,t) \sim t^{\beta-1}|x|^{-1-\frac{2\beta}{\alpha}+\frac{2}{\alpha}}$. For long times this intermediate domain covers practically the whole bulk of the distribution. For $\beta < 1 - \alpha/2$ the PDF in the center of the distribution is flat, with a Gaussian tail at $x \gg \sqrt{4K_\alpha t^\alpha}$. The results for the MSD and the PDF are reported in Table II.

Comparison of the results for renewal and nonrenewal variants of the same process shows that erasing or retaining the memory in the transport process is crucial for the features of the overall dynamics, which is the main physical consequence observed in the present work. To the best of our knowledge, SBM is the only process for which such a comparison has been performed.

ACKNOWLEDGMENTS

A.V.C. is indebted to D. Boyer for fruitful discussions which initiated this work and acknowledges the financial support from the Deutsche Forschungsgemeinschaft within Project ME1535/6-1.

[1] W. Gerstner and W. M. Kistler, *Spiking Neuron Models: Single Neurons, Populations, Plasticity* (Cambridge University Press, Cambridge, UK, 2002).

[2] S. C. Manrubia and D. H. Zanette, Phys. Rev. E **59**, 4945 (1999).

[3] M. R. Evans and S. N. Majumdar, Phys. Rev. Lett. **106**, 160601 (2011).

[4] L. Kuśmierz, S. N. Majumdar, S. Sabhapandit, and G. Schehr, Phys. Rev. Lett. **113**, 220602 (2014).

[5] L. Kuśmierz and E. Gudowska-Nowak, Phys. Rev. E **92**, 052127 (2015).
[6] S. N. Majumdar, S. Sabhapandit, and G. Schehr, Phys. Rev. E **91**, 052131 (2015).
[7] M. R. Evans and S. N. Majumdar, J. Phys. A: Math. Theor. **47**, 285001 (2014).
[8] C. Christou and A. Schadschneider, J. Phys. A: Math. Theor. **48**, 285003 (2015).
[9] A. Pal and V. V. Prasad, Phys. Rev. E **99**, 032123 (2019).
[10] A. Pal, Phys. Rev. E **91**, 012113 (2015).
[11] S. Ray, D. Mondal, and S. Reuveni, J. Phys. A: Math. Theor. **52**, 255002 (2019).
[12] M. R. Evans and S. N. Majumdar, J. Phys. A: Math. Theor. **44**, 435001 (2011).
[13] D. Boyer and C. Solis-Salas, Phys. Rev. Lett. **112**, 240601 (2014).
[14] S. N. Majumdar, S. Sabhapandit, and G. Schehr, Phys. Rev. E **92**, 052126 (2015).
[15] M. A. F. dos Santos, Physics **1**, 40 (2019).
[16] R. Falcao and M. R. Evans, J. Stat. Mech. (2017) 023204.
[17] G. J. Lapeyre and M. Dentz, Phys. Chem. Chem. Phys. **19**, 18863 (2017).
[18] I. Eliazar, Europhys. Lett. **120**, 60008 (2017).
[19] A. Pal, I. Eliazar, and S. Reuveni, Phys. Rev. Lett. **122**, 020602 (2019).
[20] R. J. Harris and H. Touchette, J. Phys. A: Math. Theor. **50**, 10LT01 (2017).
[21] S. Eule and J. J. Metzger, New J. Phys. **18**, 033006 (2016).
[22] A. Pal, A. Kundu, and M. R. Evans, J. Phys. A: Math. Theor. **49**, 225001 (2016).
[23] A. Nagar and S. Gupta, Phys. Rev. E **93**, 060102(R) (2016).
[24] X. Durang, M. Henkel, and H. Park, J. Phys. A **47**, 045002 (2014).
[25] D. Boyer, M. R. Evans, and S. N. Majumdar, J. Stat. Mech. (2017) 023208.
[26] M. Montero and J. Villarroel, Phys. Rev. E **87**, 012116 (2013).
[27] V. Méndez and D. Campos, Phys. Rev. E **93**, 022106 (2016).
[28] V. P. Shkilev, Phys. Rev. E **96**, 012126 (2017).
[29] M. Montero, A. Mas-Puigdellósas, and J. Villarroel, Eur. Phys. J. B **90**, 176 (2017).
[30] Y. Meroz and I. M. Sokolov, Phys. Rep. **573**, 1 (2015).
[31] J. Klafter and I. M. Sokolov, *First Steps in Random Walks: From Tools to Applications* (Oxford University Press, New York, 2011).
[32] I. M. Sokolov, Soft Matter **8**, 9043 (2012).
[33] R. Metzler and J. Klafter, Phys. Rep. **339**, 1 (2000).
[34] E. Barkai, Y. Garini, and R. Metzler, Phys. Today **65**(8), 29 (2012).
[35] J.-P. Bouchaud and A. Georges, Phys. Rep. **195**, 127 (1990).
[36] V. Zaburdaev, S. Denisov, and J. Klafter, Rev. Mod. Phys. **87**, 483 (2015).
[37] F. Höfling and T. Franosch, Rep. Prog. Phys. **76**, 046602 (2013).
[38] A. S. Bodrova, A. V. Chechkin, A. G. Cherstvy, and R. Metzler, New J. Phys. **17**, 063038 (2015).
[39] A. S. Bodrova, A. V. Chechkin, A. G. Cherstvy, H. Safdari, I. M. Sokolov, and R. Metzler, Sci. Rep. **6**, 30520 (2016).
[40] H. Safdari, A. G. Cherstvy, A. V. Chechkin, A. S. Bodrova, and R. Metzler, Phys. Rev. E **95**, 012120 (2017).
[41] G. K. Batchelor, Math. Proc. Cambridge Philos. Soc. **48**, 345 (1952).
[42] L. F. Richardson, Proc. R. Soc. London Sec. A **110**, 709 (1926).
[43] A. S. Monin and A. M. Yaglom, *Statistical Fluid Mechanics*, Vol. 2 (MIT Press, Cambridge, MA, 1987).
[44] M. F. Shlesinger, B. J. West, and J. Klafter, Phys. Rev. Lett. **58**, 1100 (1987).
[45] M. J. Saxton, Biophys. J. **81**, 2226 (2001).
[46] D. S. Novikov, E. Fieremans, J. H. Jensen, and J. A. Helpern, Nat. Phys. **7**, 508 (2011).
[47] D. S. Novikov, J. H. Jensen, J. A. Helpern, and E. Fieremans, Proc. Natl. Acad. Sci. USA **111**, 5088 (2014).
[48] A. Molini, P. Talkner, G. G. Katul, and A. Porporato, Physica A **390**, 1841 (2011).
[49] D. De Walle and A. Rango, *Principles of Snow Hydrology* (Cambridge University Press, Cambridge, UK, 2008).
[50] N. V. Brilliantov and T. Pöschel, *Kinetic Theory of Granular Gases* (Oxford University Press, Oxford, UK, 2004).
[51] *Granular Gases. Lecture Notes in Physics, Vol. 564*, edited by T. Poeschel and S. Luding (Springer, Berlin, 2001).
[52] *Granular Gas Dynamics. Lecture Notes in Physics, Vol. 564*, edited by T. Poeschel and S. Luding (Springer, Berlin, 2003).
[53] A. S. Bodrova, A. V. Chechkin, A. G. Cherstvy, and R. Metzler, Phys. Chem. Chem. Phys. **17**, 21791 (2015).
[54] S. C. Lim and S. V. Muniandy, Phys. Rev. E **66**, 021114 (2002).
[55] H. Safdari, A. G. Cherstvy, A. V. Chechkin, F. Thiel, I. M. Sokolov, and R. Metzler, J. Phys. A: Math. Theor. **48**, 375002 (2015).
[56] F. Thiel and I. M. Sokolov, Phys. Rev. E **89**, 012115 (2014).
[57] A. S. Bodrova, A. V. Chechkin, and I. M. Sokolov, Phys. Rev. E **100**, 012120 (2019).
[58] M. Abramowitz and I. A. Stegun, *Handbook of Mathematical Functions* (Dover, Mineola, NY, 1965).
[59] J.-H. Jeon, A. V. Chechkin, and R. Metzler, Phys. Chem. Chem. Phys. **16**, 15811 (2014).
[60] S. N. Majumdar and G. Oshanin, J. Phys. A: Math. Theor. **51**, 435001 (2018).